IJNRD.ORG ISSN : 2456-4184
INTERNATIONAL JOURNAL OF NOVEL RESEARCH AND DEVELOPMENT (IJNRD) | IJNRD.ORG
An International Open Access, Peer-reviewed, Refereed Journal

Structural and Fatigue Analysis of 3D Printed Square Blocks with Varied Materials Using Finite Element Analysis

Praveen Dhote[1st] Prakash Pandey [2nd] S.S. Chauhan [3rd]
[1]Department of Machine Design, Vaishnavi Group of Institutions, Bhopal
[2]Department of Machine Design, Vaishnavi Group of Institutions, Bhopal
[3]Department of Machine Design, Vaishnavi Group of Institutions, Bhopal

Abstract: This research paper explores the application of Finite Element Analysis (FEA) to investigate the compressive strength, fatigue life, safety factor, and natural frequencies of square blocks fabricated using different 3D printing materials. The study focuses on materials such as Thermoplastic Polyurethane (TPU), Acrylonitrile Butadiene Styrene (ABS), Polyethylene Terephthalate glycol-modified (PETG), and Polylactic Acid (PLA). The objectives include calculating alternating stress, creating layer-wise 3D CAD models, performing compressive and fatigue tests, conducting modal analysis, and comparing the results. Structural and fatigue analysis provides insights into deformation, equivalent stress, design life, safety factor, and fatigue sensitivity. The research aims to validate the FEA approach and shed light on the mechanical properties of 3D printed materials.

Index Terms **- 3D printing, Finite Element Analysis, structural analysis, fatigue analysis, natural frequencies, material properties, safety factor, additive manufacturing.**

I. INTRODUCTION

3D printing is a common term for a manufacturing process where parts are made by adding layers of material one upon other to form the final product. (Marcus Ritland 2014). When the word printer is used, most people think of a conventional printer they might use at home or in the office to print out text and images on paper. These printers print in a flat two-dimensional (2D) space using the dimensions length and width. A three-dimensional (3D) printer uses length and width but also adds depth to the print. In other word, Three-dimensional (3D) Printer is a manufacturing tool that creates physical objects from a 3D model design using an additive manufacturing method that adds layers upon layers of material. 3D prints can take almost any form, depending on the size of the printer. Afterthe initial printing process is completed, 3D prints can be linked or fused together to form larger objects. Additive Manufacturing is a general term referring to a variety of fabrication processes that use manufacturing tool to create a physical 3D object by adding material. A 3D printer is one subset of this type of manufacturing process because it continuously adds layer upon layer of material to build a physical 3D object. This is different from subtractive manufacturing that takes material away from existing resources to create an object, or the consolidation processes that take smaller parts, combines them together, and fuses them to create the designed object (S. Torta and J. Torta 2019).

1.1 Classification of 3D printing technologies

The ISO/ASTM 52900 Standard was created in 2015 to standardize all terminology as well as classify each of the different methods of 3D printing. A total of seven process categories were established. Each of these and the associated process description are explained below.

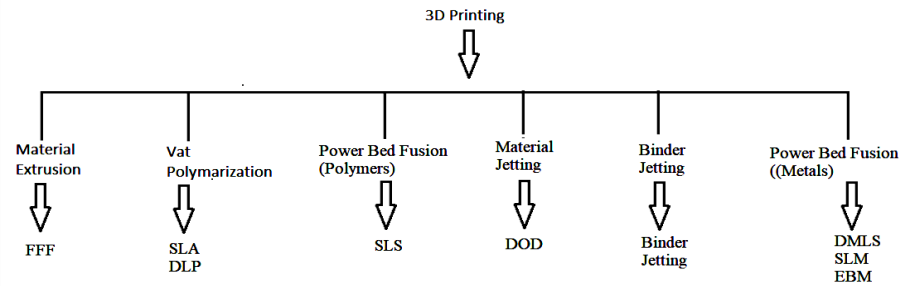

Figure 1 Classification of 3D printing technologies (Ben Redwood et. al. 2017)

1.2 Classification of 3D printing materials

3D printing materials usually come in filament, powder or resin form (depending on the 3D printing processes used). Polymers (plastics) and metals are the two main 3D printing material groups, while other materials (such as ceramics or composites) are also available. Polymers can be broken down further into thermoplastics and thermosets (3d hub, 2018).

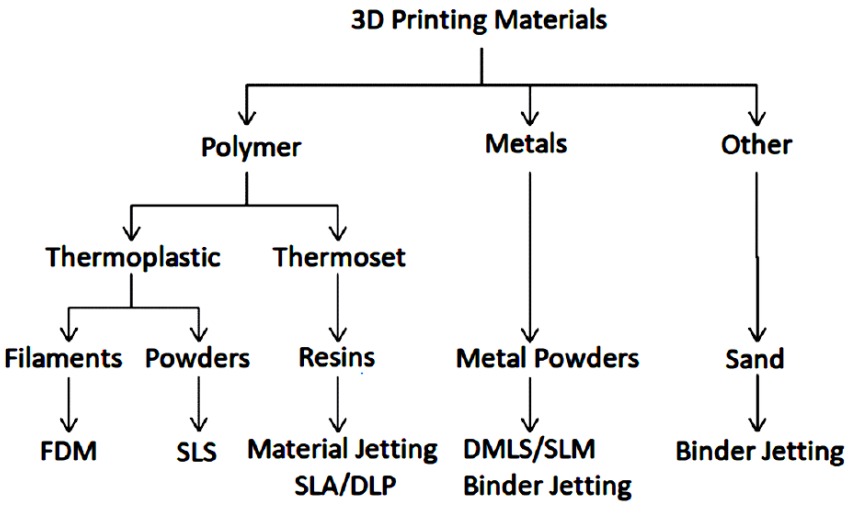

Figure 2 Classification of 3D printing materials

1.3 Advantage and limitations

Additive manufacturing (AM) is the process of additively building up a part one layer at a time. There area range of 3D printing technologies with each having their own benefits and limitations and each being able to print parts from different materials. Am technologies, corresponding base materials and advantages and disadvantages.

Table 1.3: Additive manufacturing technologies, corresponding base materials and advantages and disadvantages(Binbin He et al. 2022.)

Technology	AM process	Typical materials	Advantages	Disadvantages
Fused deposition modeling(FDM)	Material extrusion	Thermoplastics	Strong parts, complex geometries.	Poorer surface finish and slower build time than SLA.
Digital light Processing (DLP)	Vat polymerization	Liquid photopolymer.	Allows concurrent production, complex shapes and sizes high precision.	Limited product thickness, limited range of materials.
Stereolithography (SLA)	Vat polymerization	Liquid photopolymer, composites.	Complex geometries, detailed parts, smooth finish.	Post cutting required, requires support structures.
Selective laser sintering (SLS)	Powder bed fusion	Paper, plastic, metal, glass, ceramic, composites.	Requires no support structures, high heat and chemical resistant, high speed.	Accuracy limited to powder particle size, rough surface finish.
Direct metal laser sintering (DMLS)	Powder bed fusion	Stainless steel, cobalt chrome, nickel alloy.	Danse components, intricate geometries.	Needs finishing, not suitable for large parts.
Electron beam melting (EBM)	Powder bed fusion	Titanium power, cobalt chrome	Speed, less distortion of parts, less material wastage.	Needs finishing, difficult to clean the machine, caution required when dealing with X-rays.
Selective heat sintering (SHS)	Powder bed fusion	Thermoplastics powder.	Lower cost than SLS, complex geometries, no support structures required, quick turnaround.	New technology with limited track record.
Multijet modelling (MJM)	Material jetting	Photopolymers, wax.	Good accuracy and surface finish, may use multiple materials, hand free removal of support material.	Range of wax like materials is limited, relatively slow build process.

Plaster based 3D printing	Binder jetting	Bonded plaster, plaster composites	Lower price, enables color printing, high speed, excess powder can be reused.	Limited choice of materials, fragile parts.
Powder bed and inkjet head printing	Binder jetting	Ceramic powder, metal laminates, acrylic, sand, composites	Full color models, inexpensive, fast to build	Limited accuracy, poor surface finish.
Laser metal deposition	Directed energy deposition	Metals and metal alloys.	Multi-material printing capability, ability to build large parts, production flexibility.	Relatively higher cost of systems, support structures are required, need for post processing activities to obtain smooth finish.
Ultrasonic consolidation	Sheet lamination	Metal and metal alloys	Quick to make big parts, faster build speed of newer ultrasonic consolidation systems, generally non-toxic materials.	Parts with relatively less accuracy and inconsistent quality compared to other AM processes, need for post processing.
Laminated object manufacturing	Sheet lamination	Paper, plastic, metal laminates, ceramics, composites.	Relatively less expensive, nontoxic materials, quick to make big parts.	Less accurate, non-homogenous parts.

Parts can be produced in almost any geometry, which is one of the core strengths of 3D printing. Also, 3D printing does not rely on expensive tooling having essentially no start-up costs. The advantage of this is the rapid verification and development of prototypes and low volume production parts.
One of the biggest limitations of 3D printing is the inability to produce parts with material properties equivalent to those made via neither subtractive nor formative techniques.

II LITERATURE REVIEW

Binbin He et al. (2022) Corneal regeneration has been a longstanding challenge due to the cornea's intricate structure and issues with hepatocyte transformation. To address this, researchers are turning to 3D printing to create a biomimetic implant that mimics the cornea's natural layers. Utilizing a blend of Gelatin methacrylate (GelMA) and long-chain poly(ethylene glycol) diacrylate (PEGDA) as the ink, the Digital Light Processing (DLP) printing technology can produce mechanically robust PEGDA-GelMA structures. These printed hydrogels offer multiple advantages: they foster cell adhesion, proliferation, and migration, exhibit high light transmittance, and provide an optimal swelling degree, nutrient permeability, and degradation rate. This breakthrough 3D-printed approach holds promise in revolutionizing corneal regeneration, offering a harmonious blend of structure and function. Recent advancements in 3D printing have led to the development of an innovative bi-layer dome-shaped corneal scaffold. This scaffold integrates two distinct layers: a top layer embedded with rabbit corneal epithelial cells (rCECs) to mimic the cornea's epithelia and a bottom layer laden with rabbit adipose-derived mesenchymal stem cells (rASCs) that replicates the cornea's fibrous stroma with an orthogonally aligned orientation. When tested in a rabbit keratoplasty model, this scaffold showcased remarkable post-operative results, including effective sealing of corneal defects, re-epithelialization, and stromal regeneration. The success can be attributed to the 3D printed scaffold's precise microstructure combined with the strategic placement of cells, creating an optimal environment for corneal healing and regeneration.

Chao Bao et al. (2022) Compared with conventional von Neumann's architecture-based processors, neuromorphic systems provide energy-saving in-memory computing. The 3D neuromorphic humanoid hand represents a pioneering blend of biology and robotics, aiming to simulate human reflexes in an artificial system. Designed to provide unconscious responses based on prior training, the hand mimics the human reflex arc, processing intricate spatiotemporal data swiftly. It's constructed from a 3D structural design, integrated with 3D-printed pressure sensors, and powered by a portable neuromorphic device crafted using advanced multi-axis robot 3D printing technology. The result is a robotic hand capable of bioinspired signal perception and processing, automatically adjusting its grip on unfamiliar objects without the need for a traditional control processor. This innovation offers a glimpse into a future of more autonomous and bioinspired robotic systems.

Farah Syazwani Shahar et al (2022) The surging demand for ankle-foot orthosis (AFO) has catalyzed the adoption of 3D printing in its production due to the technology's speed, design optimization, and cost benefits. A shift toward eco-friendly alternatives has prompted researchers to explore the use of natural composites like kenaf—a fibrous tropical plant—blended with Polylactic Acid (PLA), a biodegradable polymer, as a 3D printer filament. This fusion aims not only to enhance the AFO's sustainability but also

to decrease its weight and material costs. However, given the everyday use of AFOs, it's imperative to rigorously evaluate the composite's density, fatigue, and impact strengths to ensure user safety and durability. This research endeavors to scrutinize the kenaf/PLA composite's suitability for AFO production, bridging the gap between sustainability and user-centric design. In a study exploring the potential of kenaf/PLA composite for 3D printed ankle-foot orthosis (AFO), the kenaf filler was varied at concentrations of 3, 5, and 7 wt. %. Upon extruding these composites into filaments for 3D printing, it was observed that as the filler content increased, there was a notable decrease in both the density and impact resistance of the printed specimens. However, the fatigue life saw a significant improvement, indicating enhanced durability with increased filler amounts. This inverse relationship between density and fatigue life suggests the kenaf/PLA composite, with its ability to achieve a balance between reduced weight and increased durability, holds promise as an effective and sustainable material for AFO production.

Irina Ivanova et al (2022) comparative analysis of various indirect techniques to evaluate the buildability of 3D printed cement-based materials. The methods scrutinized encompass the constant rotational velocity (CRV) or constant shear rate (CSR) test implemented through rotational rheometry, the established unconfined uniaxial compression test (UUCT), along with the introduction of the confined uniaxial compression test (CUCT), and the fast penetration test. To ensure a comprehensive examination, the experimental phase incorporated extruded samples from six distinctive printable mortars and two unique printable concretes. These samples exhibited a diverse range of rheological behaviors, brought about by the inclusion of an array of additives and admixtures. In the interest of gauging the efficacy of the indirect techniques, predictions regarding the potential failures of the material, especially the stability failure in hollow cylindrical designs, were made. These predictions were then juxtaposed with findings from the direct printing test. The study goes a step further by not just highlighting the comparative benefits and pitfalls of each test method but also contemplating the practicality and feasibility of integrating these methods into automated, real-time monitoring systems, ensuring optimal buildability during the 3D printing process.

Philippe Lesage et al (2022) we delve into the dynamical properties of mechanical constructs produced through the Selective Laser Melting (SLM) technique, paying particular attention to different manufacturing orientations. For a more comprehensive analysis, these additive manufactured samples are compared with components produced through subtractive manufacturing methods. The metallic samples, created additively, were meticulously fabricated using the Renishaw AM 250 3D printer, a state-of-the-art piece of equipment from Renishaw. The evaluation procedure employed a unique approach: vibration analysis of the embedded-free beam installation. This experimental configuration was systematically recreated, ensuring consistent geometry across samples, irrespective of their printing orientations. These samples were then subjected to low-velocity impact tests. The inclusion of accelerometers in the setup proved instrumental, as they captured the mechanical reactions of every specimen in real-time. These readings facilitated a deep dive into understanding the intricate dynamical behaviors exhibited by each component. Furthermore, a critical aspect of the study was discerning the influence of both the printing orientation and the specific angles utilized during the SLM process on the dynamical properties of the resultant structures.

Saquib Rouf et al (2022) 3D printing, over recent years, has emerged as a groundbreaking technology with the potential to revolutionize the fabrication of industrial components. Intriguingly, while this technology promises a myriad of advantages, the intrinsic methodology it employs has cast a spotlight on the mechanical strength of 3D printed items, propelling it to the forefront of academic and industrial research. The undeniable economic and technical efficiencies 3D printing brings to the table position it as a viable contender to supplant traditional manufacturing methods, especially when it comes to crafting intricate and highly-optimized designs. This manuscript delves deep into the multifaceted realm of 3D printing techniques that cater to industrial applications. Within its scope, it meticulously examines the assorted process parameters native to each method and their consequential impact on the mechanical attributes of the fabricated components. This includes a thorough assessment of fatigue resistance, tensile strength, bending resilience, and other crucial properties, with a special emphasis on parts made of polymeric materials. In addition to this, the paper underscores the tribological characteristics - a pivotal but often underexplored facet of 3D printed components. To furnish readers with a holistic perspective, a systematic review of existing literature concerning these themes is incorporated. The practical applications of such 3D creations are vast, spanning sectors like medical, aerospace, and automotive, all of which are elaborated upon in dedicated segments. Complementing this, there's an exploration into the environmental sustainability of 3D printed parts, emphasizing their eco-friendly potential. Wrapping up, the document provides insights into promising avenues for future investigations, proffers valuable recommendations, and candidly addresses the challenges and intricacies that accompany the evolution and adoption of 3D printing in contemporary manufacturing scenarios.

Su Hyun Lee et al (2022) Recently, pet food, particularly dental hygiene chews for dogs and cats, has gained prominence as a supplementary method for promoting oral health. Such chews provide pet owners a straightforward means to maintain their pets' dental hygiene at home, offering a proactive solution against teeth build up and plaque. Dental chews, specifically, play a pivotal role in curtailing plaque, employing either chemical or mechanical techniques. Recognizing the potential to enhance the effectiveness of these chews, this study ventured into the realm of 3D printing, aiming to customize chews that align with individual dogs' dental anatomy and tastes. This research delved deep into devising optimal methodologies for crafting these dental hygiene chews, utilizing a combination of corn starch and glycer in as the primary components for an extrusion-based 3D printing process. Notably, as glycer in content was incremented, there was a noticeable uptick in the viscoelastic properties of the dental chews. To ascertain the optimal texture and plaque-removal prowess, an extensive evaluation was undertaken using a texture analyser and dog dentures, factoring in variables such as the infill level (ranging from 40%, 60%, to 80%) and varied glycer in concentrations. Results showcased that chews with a 60% infill, combined with 10% and 20% glycer in content, were the frontrunners in plaque eradication, proving particularly effective on both canine teeth and premolars. Additionally, design intricacies were also assessed: a lattice design, characterized by square cavities, was exceptionally adept for canine teeth. In contrast, a more fragmented, crumbly texture showed enhanced efficacy for the premolars.

A.K. Haldar et al (2021) looks at 3D printed sandwich panels with special wave-like designs, testing them under pressure. We mainly studied two unique shapes in the middle of these panels: triangular and trapezoidal. We checked how changes in thickness,

outer layers, height of the middle section, and the connection between layers affected their strength. For the printing, we used an eco-friendly material combined with small carbon fibers. Our tests showed that when the middle section was thicker, the panels were stronger and absorbed more energy. Also, a larger connection area between the layers made the panels even stronger.

III. OBJECTIVE

3D printing technology is an additive manufacturing process that creates three-dimensional solid objects from a digital file. In this process, layers of material are printed until a complete object is formed using a 3D printer. The use of 3D printing makes it possible to produce even complex geometries with minimal waste of materials compared to conventional fabrication. The main objective to this present work to investigate the compressive strength, fatigue life, safety factor and natural frequencies of the square block for 3D printing using different materials.

There are following objective of the present work.

- To calculate alternating stress for different materials used in this work such as Thermoplastic Polyurethane (TPU), Acrylonitrile Butadiene Styrene (ABS), and Polyethylene Terephthalate glycol-modified (PETG) and Polylactic Acid (PLA).
- To create layer wise three dimensional CAD model using ACP (Pre) for FEM analysis.
- To perform compressive test using structural analysis for different orientation using four different 3D printing materials to investigate the total deformation and equivalent stress layer wise.
- To perform fatigue analysis to investigate the fatigue life and safety factor by using fatigue tool.
- To perform the Model analysis to check the natural frequencies with six possible modes.
- Compare the results obtained from the above analysis and validate with the base paper.

IV. METHODOLOGY

3D printing makes designs easier and allows engineers to create prototypes and mock-ups of faster than ever before. Editing can be made easily and can also choose best of all quickly. The replace ability of conventional manufacturing technology with 3D printing with great accuracy can be possible. In the present work square block of 25 mm x 25 mm x 25 mm has been used to perform structural, fatigue and model analysis for different types of 3D printing materials such as TPU, ABS, PLA & PEGT. In the present work finite element analysis have been conducted on Simple structure of square block with dimensional parameter 25 mm x 25 mm x 25 mm, this FEM analysis includes compression test using static structural analysis, fatigue analysis and model analysis. The total deformation and equivalent stress layer wise have been found by compression test, whereas the design life and safety factor of the material is determined by the fatigue analysis and the natural frequency of the square block has been found in the modal analysis. The materials used in the present work are Thermoplastic Polyurethane (TPU), Acrylonitrile Butadiene Styrene (ABS), Polyethylene Terephthalate glycol-modified (PETG) and Polylactic Acid (PLA).

Table 4.1: Material properties *[https://matweb.com/]*

Property	**TPU**	**ABS**	**PLA**	**PETG**
Density [Kg/m^3]	1660	1040	1290	1290
Coefficient of thermal expansion	11x10^{-6}	72x10^{-6}	27x10^{-6}	68x10^{-6}
Young Modulus GPa	5.50	2.3	4.8	2.1
Poisson's Ratio	0.3897	0.3	0.3	0.3
Bulk modulus [MPa]	8.3107E+6	109167E+9	4E+9	1.75E+9
Shear modulus [MPa]	1.9788E+6	8.8462E+8	1.846E+9	8.0769E+8
Tensile Yield strength [MPa]	79.3	35.9	57.9	53
Tensile Ultimate strength [MPa]	96	26.4	47.9	45.8

4.1 Calculation of Bulk modulus and shear modulus

Bulk modulus

$E = 3k(1 - 2\nu)$

$K = \frac{E}{3(1-2\nu)}$

Where:

E = Young modulus

K = Bulk Modulus

ν = Poisson's ratio

Shear Modulus:

$G = \frac{1}{2}\left(\frac{E}{1+\nu}\right)$

Where:

G = Shear modulus

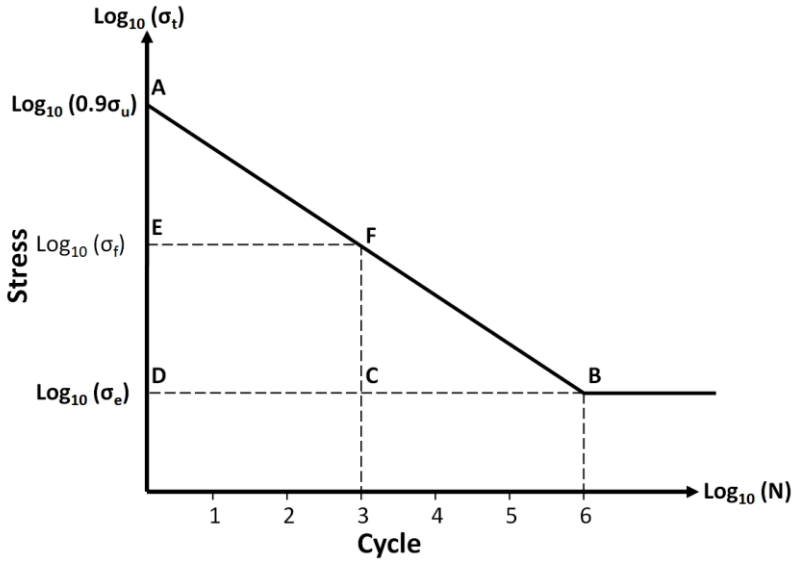

Figure 3 S-N curve

4.2 Calculation of fatigue strength at different cycle

$$Log_{10}(\sigma_f) = Log_{10}(0.9\sigma_u) - \frac{Log_{10}(0.9\sigma_u) - Log_{10}(\sigma_e)}{Log_{10}(10^6) - Log_{10}(10)} \times [Log_{10}(N) - Log_{10}(10)]$$

$$\sigma_e = 0.3\sigma_u$$

σ_u for TPU = 86.4 MPa — σ_e for TPU = 25.92 MPa
σ_u for ABS = 26.4 MPa — σ_e for ABS = 7.38 MPa
σ_u for PLA = 47.9 MPa — σ_e for PLA = 14.37 MPa
σ_u for PETG = 45.8 MPa — σ_e for PETG = 13.74 MPa

Table 4.2: Calculation of alternating stress for different materials

Cycle	Log10 (N)	Alternating Stress TPU [MPa]	Alternating Stress ABS [MPa]	Alternating Stress PLA [MPa]	Alternating Stress PETG [MPa]
10	1	86.39	23.76	43.11	41.22
20	1.3	80.89	22.15	35.42	33.94
50	1.699	74.25	20.18	27.28	26.21
100	2.0	69.36	18.81	22.40	21.56
200	2.3	64.94	17.53	18.41	17.75
2000	3.3	52.13	13.88	9.57	9.29
10000	4	44.67	11.78	6.05	5.90
20000	4.3	41.85	10.98	4.97	4.86
1E+5	5	35.88	9.32	3.15	3.09
2E+5	5.3	33.59	8.69	2.58	2.54
1E+6	6	28.80	7.38	1.63	1.62

4.3 Introduction of Finite Element Analysis

Structural analysis

Structural analysis is a fundamental engineering discipline that plays a pivotal role in assessing and comprehending the behavior of structures or components under various loads and conditions. It serves as a crucial tool for engineers and designers to predict and understand the displacements, stresses, strains, and internal forces experienced by these structures. This analytical process is particularly valuable when dealing with loads that do not induce substantial inertia and damping effects.

Modal analysis

Modal analysis is a crucial engineering technique employed to discern the vibration traits of a structure or a machine component, primarily focusing on identifying their natural frequencies and corresponding mode shapes. These insights gleaned from modal analysis serve as a foundational knowledge base for a spectrum of subsequent analyses. For instance, in contact analysis, modal analysis can identify unconstrained bodies, and in transient analysis, it assists in determining the appropriate time-step size.

Fatigue Analysis

Fatigue is a process of the cycle-by-cycle accumulation of damage in a material undergoing fluctuating stresses and strains. A main feature of fatigue is that the load is not large enough to cause global plastic deformation or immediate failure. Instead, failure occurs after a component has experienced a certain number of load fluctuations, that is, after the accumulated damage has reached a critical level.

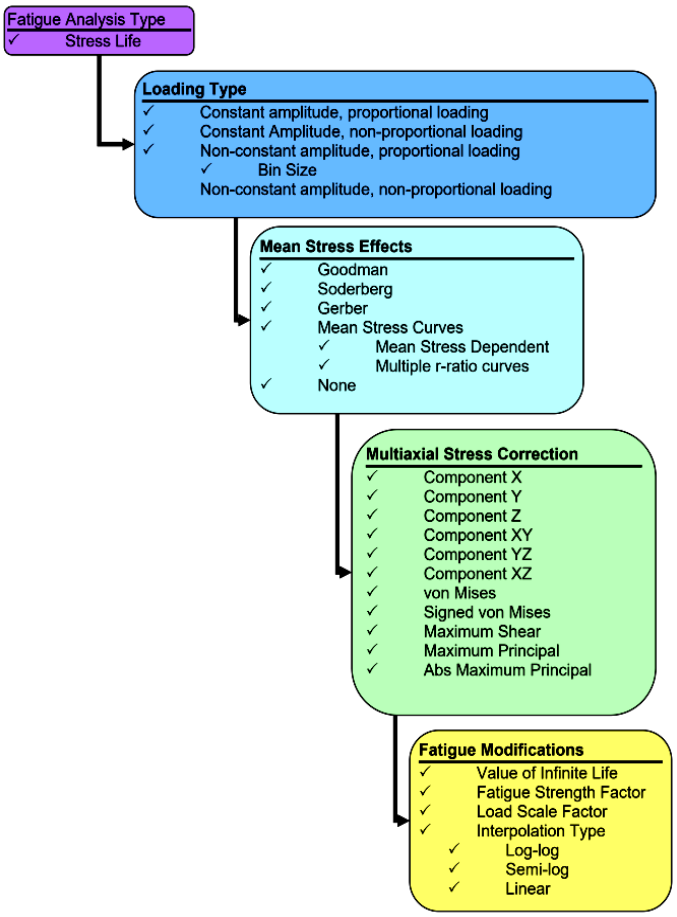

Figure 4 Fatigue analysis type stress life decision tree

4.4 Mean stress corrections for stress life:

For Stress Life at different mean stresses or r-ratio's mean stress can be accounted for directly through interpolation between material curves or several empirical options may be used such as Gerber, Goodman and Soderberg theories which use static material properties along with S-N data to account for any mean stress.

$$Soderberg\ Equation = \frac{\sigma_{Alternating}}{S_{Endurance\ limit}} + \frac{\sigma_{mean}}{S_{Yield\ strength}} = 1$$

$$Goodman\ Equation = \frac{\sigma_{Alternating}}{S_{Endurance\ limit}} + \frac{\sigma_{mean}}{S_{ultimate\ strength}} = 1$$

$$Gerber\ Equation = \frac{\sigma_{Alternating}}{S_{Endurance\ limit}} + \left(\frac{\sigma_{mean}}{S_{ultimate\ strength}}\right)^2 = 1$$

4.5 General Fatigue Results

Fatigue Life: The available life for the specified fatigue analysis is visually presented across the entire model, similar to any other contour result. In the case of constant-amplitude loading, this value signifies the number of cycles the component can endure before experiencing fatigue-induced failure. In situations where the loading is non-constant, the available life is representative of the number of loading blocks the component can withstand before reaching failure.

Fatigue Damage: The presented contour plot illustrates fatigue damage concerning a specified design life. Fatigue damage is a parameter calculated by dividing the design life by the available life. In this context, it's essential to understand that when the values on this plot exceed 1, it serves as a clear indication that structural failure is expected to occur prior to reaching the intended design life.

Fatigue Safety Factor: The provided graphical representation is a contour plot depicting the factor of safety concerning the potential occurrence of fatigue failure over a designated design life. Within this graphical representation, the maximum attainable Factor of Safety is capped at a value of 15. It's crucial to note that, in the context of the Fatigue Safety Factor, any values that fall below the threshold of one serve as a clear indicator of structural failure occurring prior to the completion of the intended design life.

Biaxiality Indication: In the realm of mechanics and stress analysis, the concept of biaxiality indication serves as a pivotal parameter for characterizing stress states within materials and structures. This metric is precisely defined as the ratio between the smaller principal stress and the larger principal stress, with the critical stipulation that the principal stress nearest to zero is disregarded in this calculation. Biaxiality indication assumes values across a spectrum that encapsulates various stress conditions.

Fatigue Sensitivity: shows how the fatigue results change as a function of the loading at the critical location on the model. Sensitivity may be found for life, damage, or factor of safety. Linear, Log-X, Log-Y, or Log-Log scaling can be chosen for chart display. Default values for the sensitivity options may be set through the Control Panel.

4.6 Algorithm used for Finite element analysis of Structural and fatigue analysis

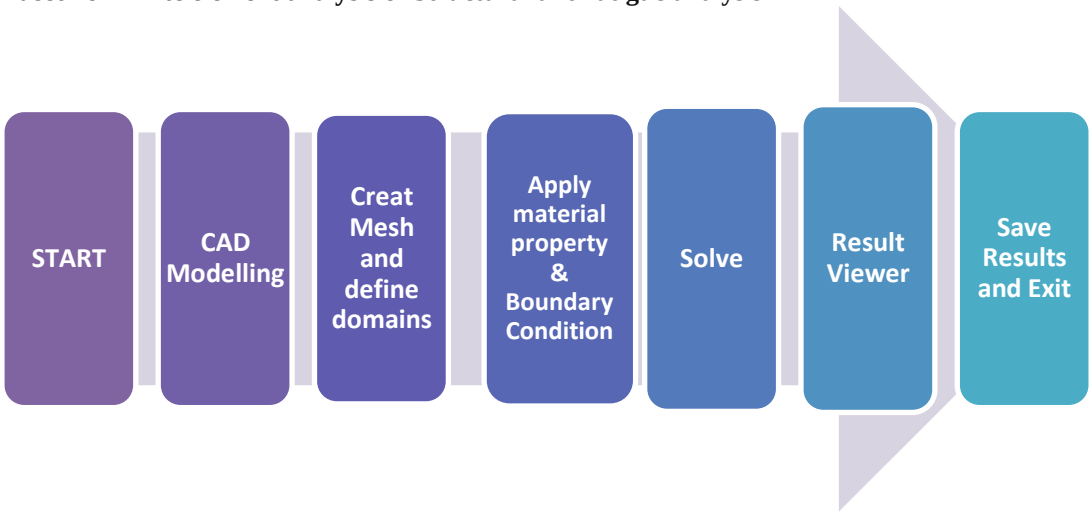

Figure 5. Algorithm used for Finite element analysis of Structural and fatigue analysis

4.7 Validation of work

For the validation of present work the dimensional parameter for the square block is taken from a research paper of *D.W. Abbot et al. (2019) "Finite Element Analysis of 3D Printed Model via Compression Tests" Procedia Manufacturing, Volume 35, 2019, Pages 164-173. doi.org/10.1016/j.promfg.2019.06.001.*

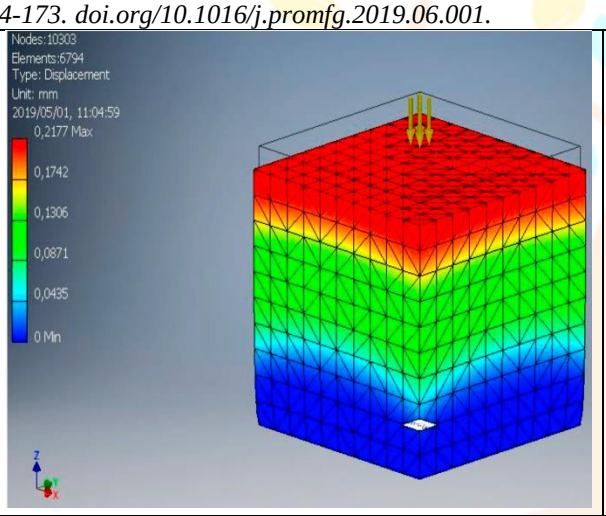

Figure 6(a): Total deformation of square block for ABS at 122500 N applied in vertical direction [D.W abbot (2019)]

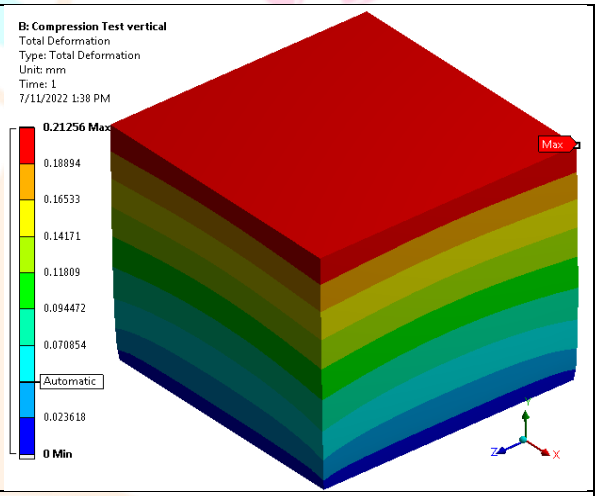

Figure 6(b): Total deformation of square block for ABS at 122500 N applied in vertical direction Material [Present work]

From the above contour diagram it has been observed that when the vertical load is applied at the top of the square block for ABS material, the maximum deformation of 0.2177 mm obtained by *D.W abbot (2019)*, while in the present work the maximum deformation of 0.21256 mm obtained with 2.42% variation as compared with published research paper.

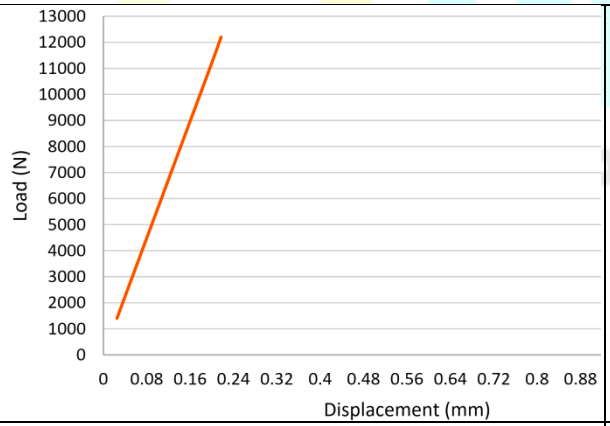

Figure 7 (a): Applied load Vs Displacement results obtained from FEM analysis for ABS Material [D.W abbot (2019)]

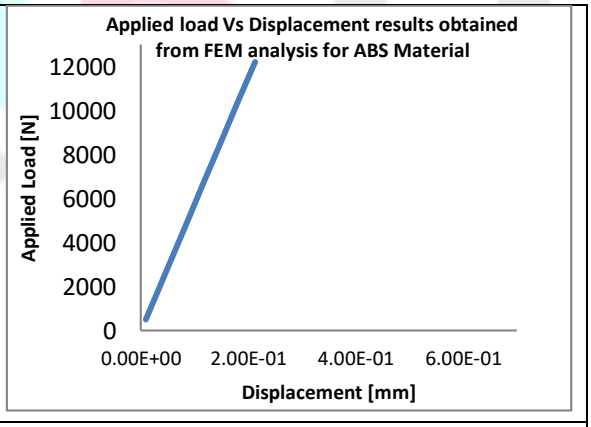

Figure 7 (b): Applied load Vs Displacement results obtained from FEM analysis for ABS Material [Present work]

From the above graph it has been observed that the displacement is a straight line, which shows that the load is directly proportional to the displacement. The maximum displacement of 0.21256 mm at maximum compressive load of 12200 N in vertical direction for ABS material as shown in the figure.

After validation of present work for the ABS material, FEM analysis has been performed for different materials such as TPU, PLA & PETG with the applied load in both vertical and horizontal directions. In this work, fatigue analysis and model analysis were also performed to check the material stability of the mentioned materials.

3.3 Theoretical framework

Variables of the study contains dependent and independent variable. The study used pre-specified method for the selection ofvariables. The study used the Stock returns are as dependent variable. From the share price of the firm the Stock returns are calculated. Rate of a stock salable at stock market is known as stock price.

V. RESEARCH METHODOLOGY

In the present work finite element analysis have been conducted on Simple structure of square block with dimensional parameter 25 mm x 25 mm x 25 mm, this FEM analysis includes compression test using static structural analysis, fatigue analysis and model analysis. The total deformation and equivalent stress layer wise have been found by compression test, whereas the design life and safety factor of the material is determined by the fatigue analysis and the natural frequency of the square block has been found in the modal analysis. The materials used in the present work are Thermoplastic Polyurethane (TPU), Acrylonitrile Butadiene Styrene (ABS), Polyethylene Terephthalate glycol-modified (PETG) and Polylactic Acid (PLA). For the creation of square block ACP-pre is use where block has been created by combining two or more layered materials.

5.1 Comparative result of Total deformation at vertical loading for different materials

Applied Compressive Load [N]	Total deformation at vertical loading for TPU [mm]	Total deformation at vertical loading for ABS [mm]	Total deformation at vertical loading for PLA [mm]	Total deformation at vertical loading for PETG [mm]
-1220	3.62E-03	8.71E-03	4.17E-03	9.50E-03
-2440	8.70E-03	1.74E-02	8.35E-03	1.90E-02
-3660	1.38E-02	3.14E-02	1.50E-02	3.42E-02
-4880	1.96E-02	4.70E-02	2.25E-02	5.13E-02
-6100	2.75E-02	6.62E-02	3.17E-02	7.22E-02
-7320	3.77E-02	9.06E-02	4.34E-02	9.88E-02
-8540	4.93E-02	1.18E-01	5.68E-02	1.29E-01
-9760	6.16E-02	1.48E-01	7.10E-02	1.62E-01
-10980	7.47E-02	1.79E-01	8.60E-02	1.96E-01
-12200	8.84E-02	2.13E-01	1.02E-01	2.32E-01

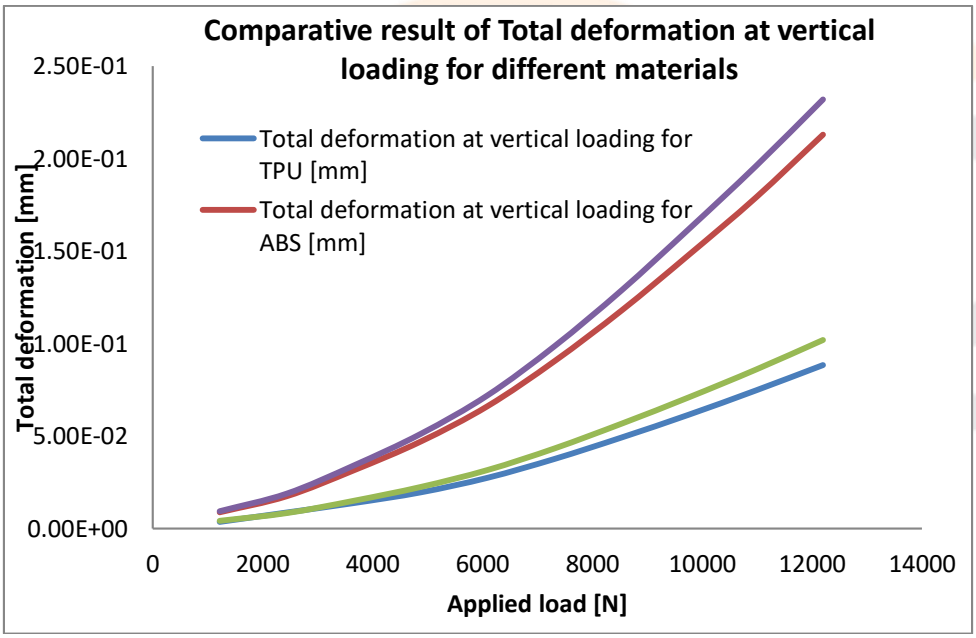

Figure 8 Comparative result of Total deformation at vertical loading for different materials

5.2 Comparative result of Total deformation at horizontal loading for different materials

Applied Compressive Load [N]	Total deformation at horizontal loading for TPU [mm]	Total deformation at horizontal loading for ABS [mm]	Total deformation at horizontal loading for PLA [mm]	Total deformation at horizontal loading for PETG [mm]
1220	3.63E-03	8.71E-03	4.18E-03	9.50E-03
2440	7.25E-03	1.74E-02	8.35E-03	1.90E-02
3660	1.31E-02	3.14E-02	1.50E-02	3.42E-02
4880	1.96E-02	4.71E-02	2.25E-02	5.13E-02
6100	2.76E-02	6.62E-02	3.17E-02	7.22E-02
7320	3.77E-02	9.06E-02	4.34E-02	9.89E-02
8540	4.93E-02	1.19E-01	5.68E-02	1.29E-01
9760	6.17E-02	1.48E-01	7.10E-02	1.62E-01
10980	7.47E-02	1.80E-01	8.60E-02	1.96E-01
12200	8.85E-02	2.13E-01	1.02E-01	2.32E-01

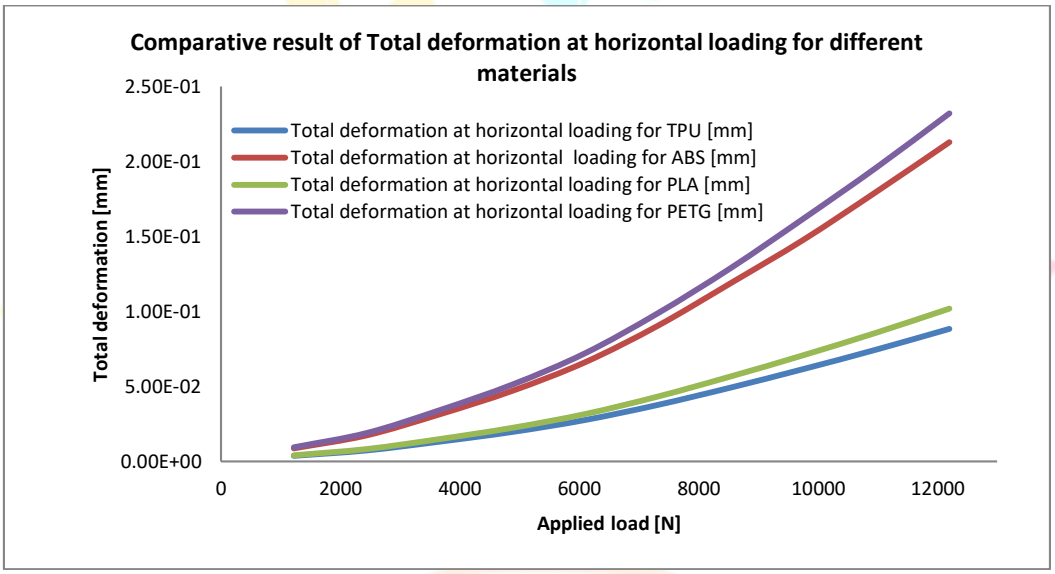

Figure 9 Comparative result of Total deformation at horizontal loading for different materials

5.3 Results analysis of Equivalent stress layer wise for different material:

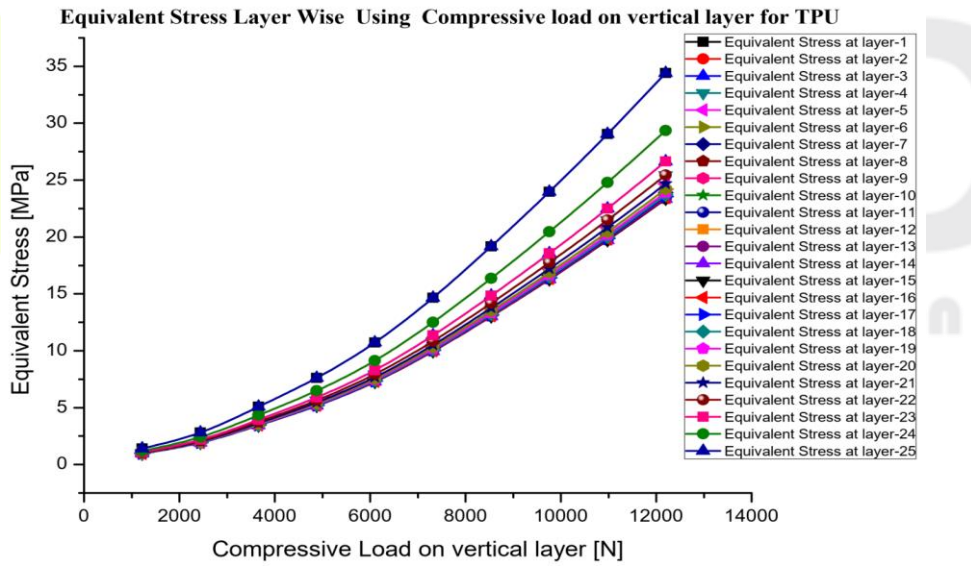

Figure 10 Equivalent stress layer wise using compressive load on vertical layer for TPU

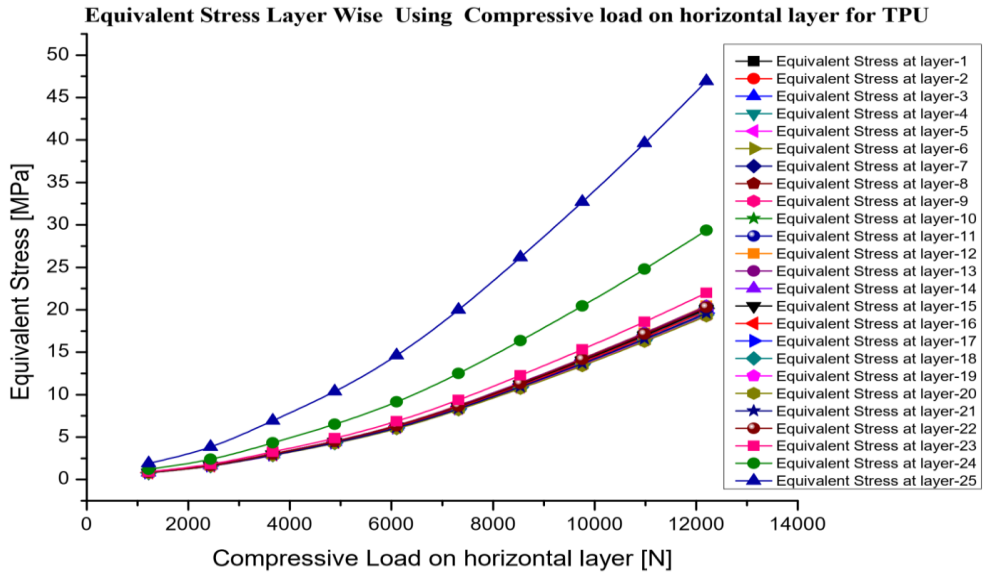

Figure 11 Equivalent stress layer wise using compressive load on horizontal layer for TPU

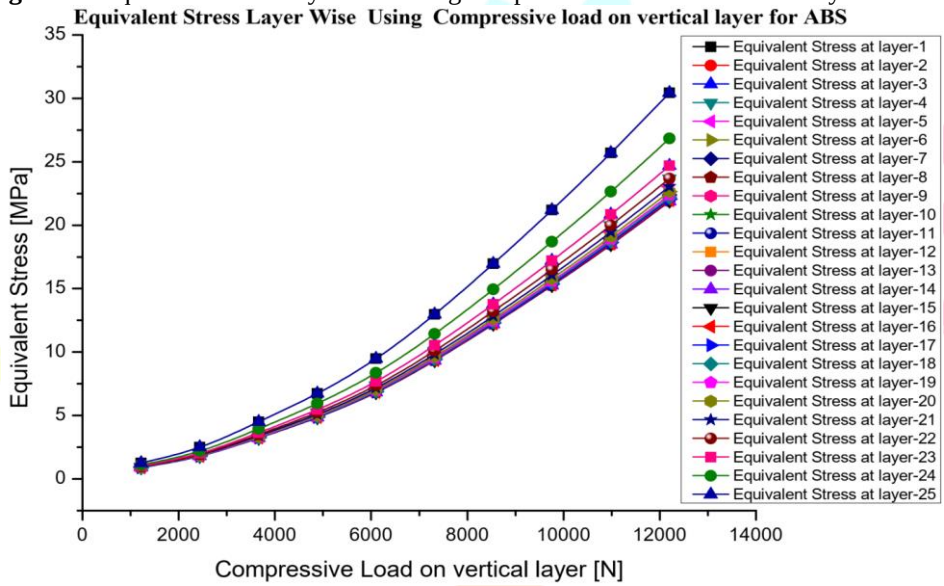

Figure 12 Equivalent stress layer wise using compressive load on vertical layer for ABS

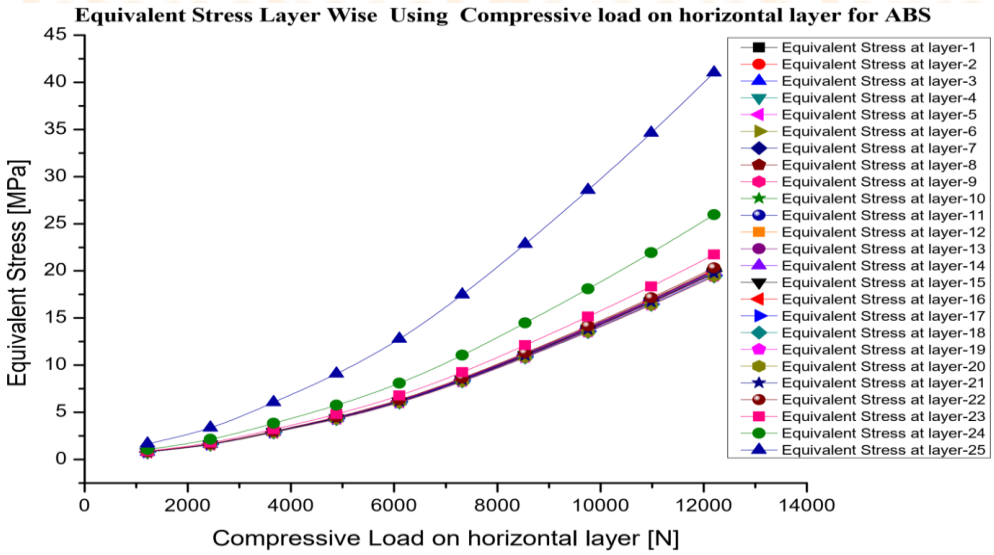

Figure 13 Equivalent stress layer wise using compressive load on horizontal layer for ABS

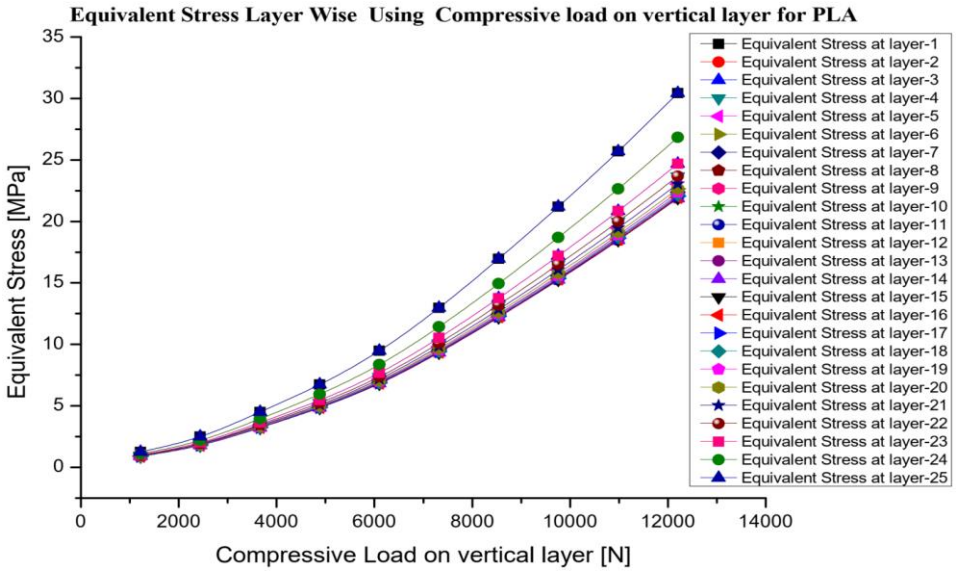

Figure 14 Equivalent stress layer wise using compressive load on vertical layer for PLA

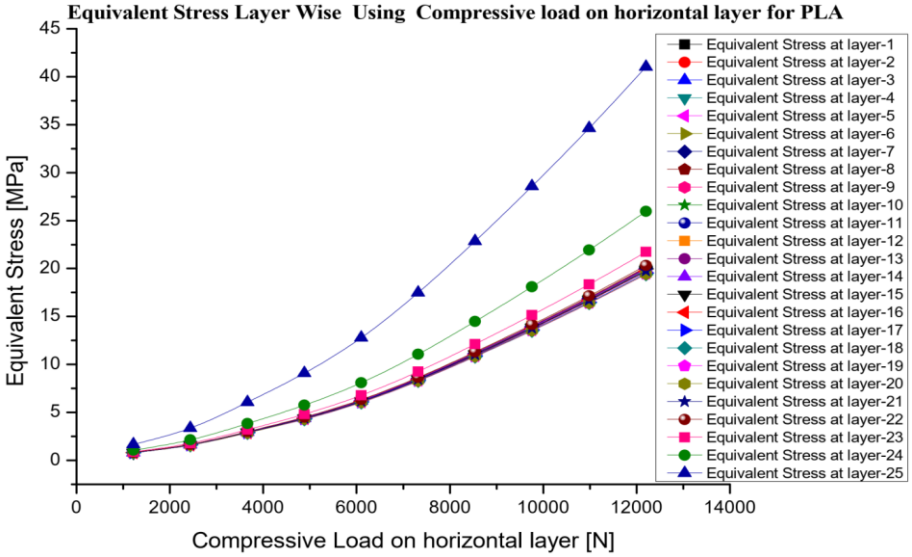

Figure 15 Equivalent stress layer wise using compressive load on horizontal layer for PLA

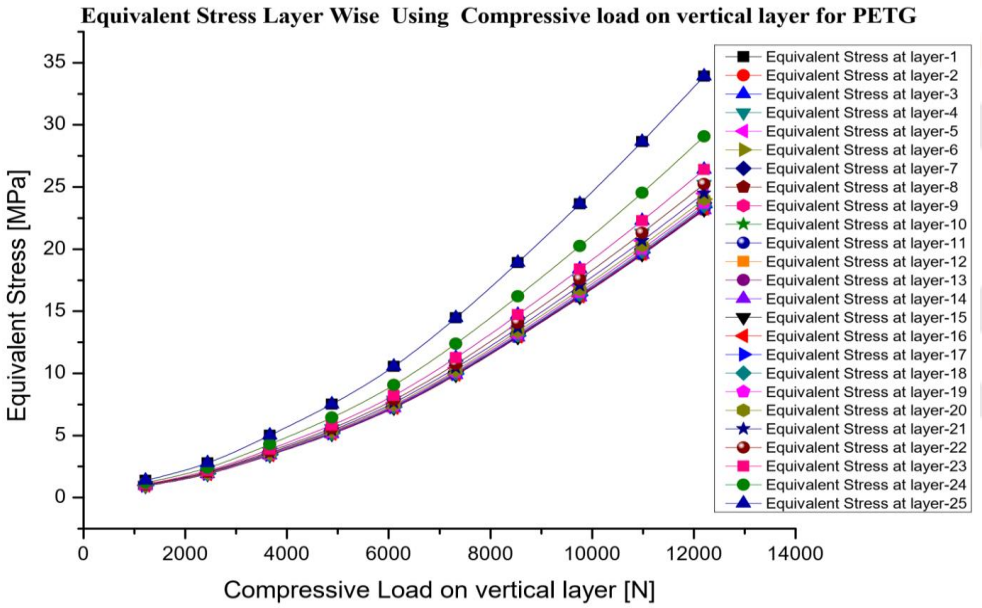

Figure 16 Equivalent stress layer wise using compressive load on vertical layer for PETG

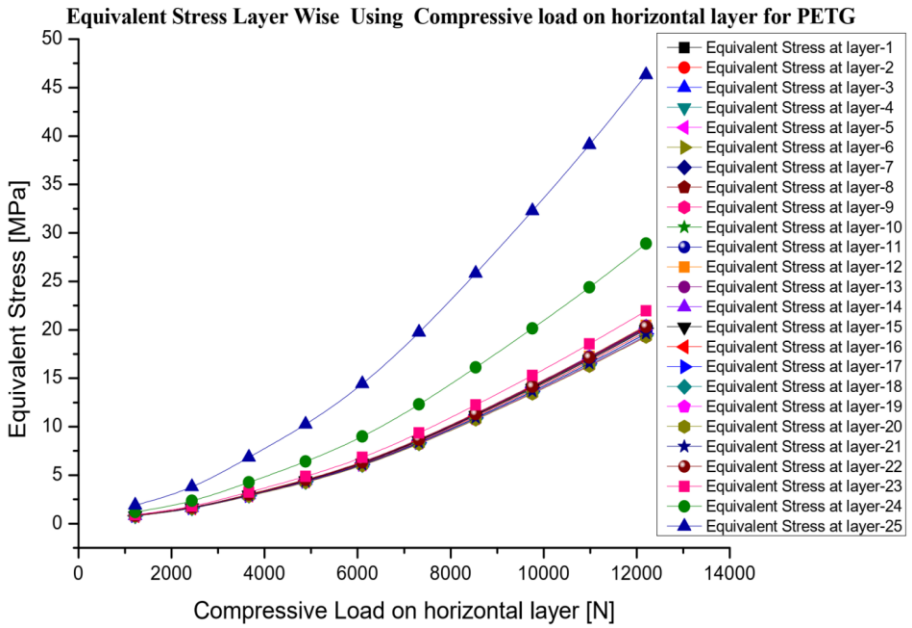

Figure 17 Equivalent stress layer wise using compressive load on horizontal layer for PETG

5.4 Comparative result of maximum equivalent stress for different materials

Materials	Maximum equivalent stress at load on vertical Layer [MPa]	Maximum equivalent stress at load on horizontal Layer [MPa]
TPU	34.406	46.933
ABS	30.425	40.016
PLA	30.425	41.016
PETG	33.93	46.317

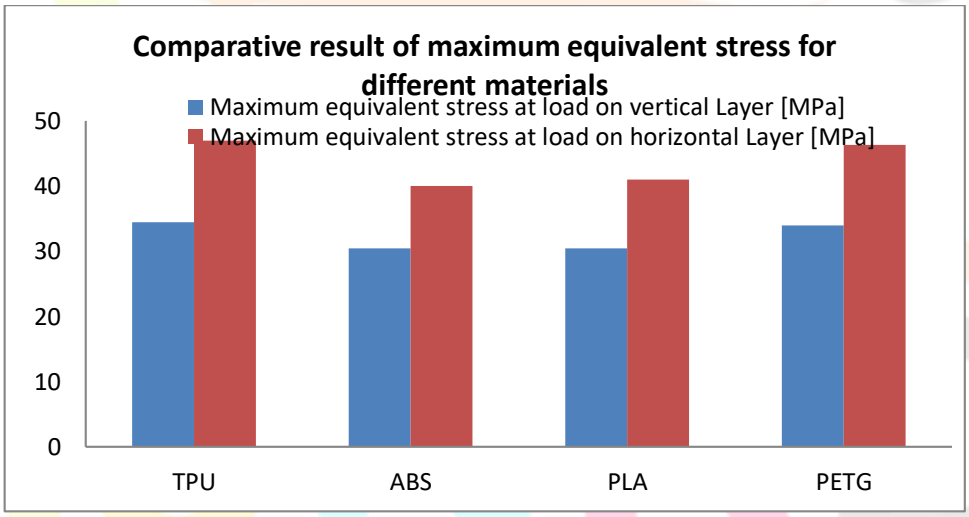

Figure 18 Comparative result of maximum equivalent stress for different materials

5.5 Comparative result of Fatigue life for different materials

Materials	Fatigue life at load on vertical Layer	Fatigue life at load on horizontal Layer
TPU	6.065E+5	7.8125E+5
ABS	5.391E+6	6.8432E+6
PLA	1250.4	1362.3
PETG	5.725E+5	6.1688E+5

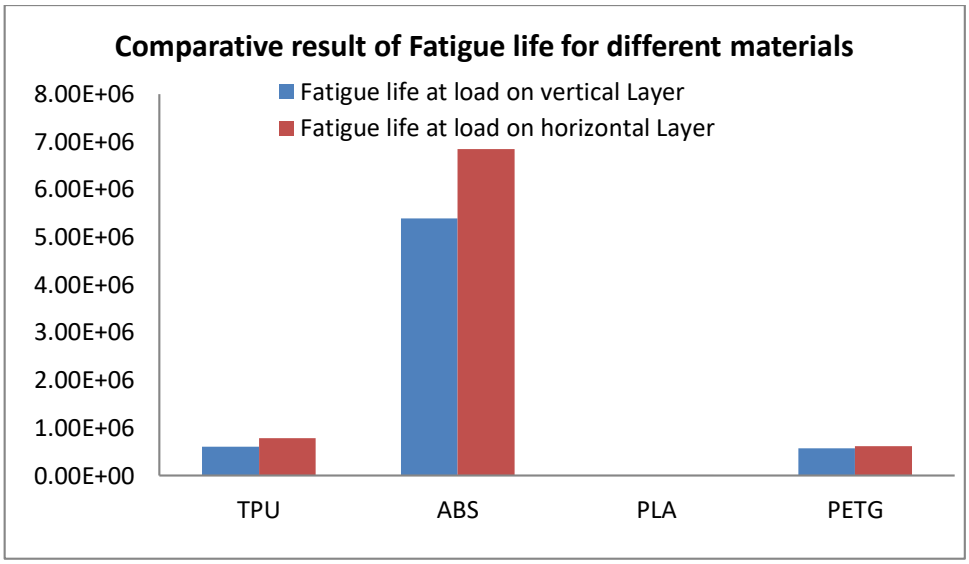

Figure 19 Comparative result of Fatigue life for different materials

5.6 Comparative result of safety factor for different materials

Materials	Safety factor at load on vertical Layer	Safety factor at load on horizontal Layer
TPU	0.6145	0.6296
ABS	0.18239	0.18687
PLA	0.04028	0.041274
PETG	0.035116	0.035979

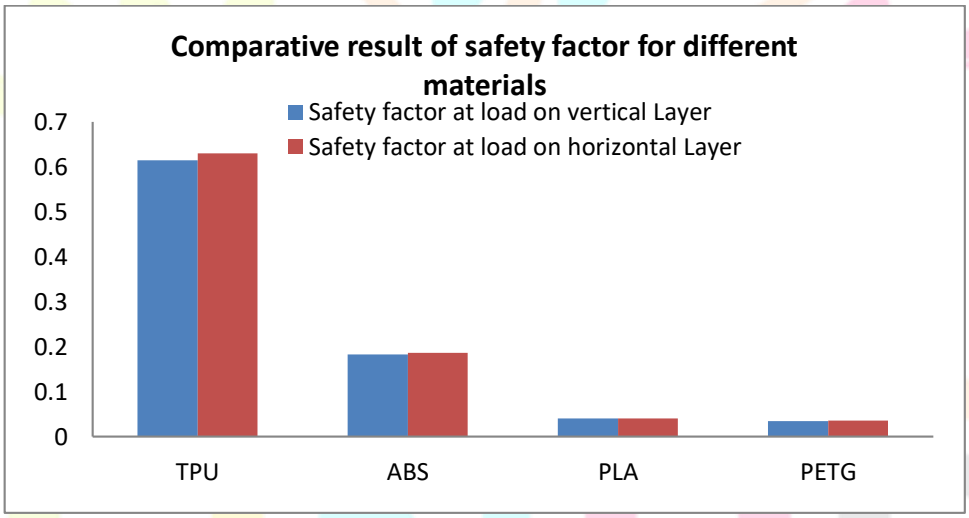

Figure 20 Comparative result of safety factor for different materials

6. CONCLUSION

This study utilized Finite Element Analysis (FEA) to assess the mechanical properties of square blocks created with diverse 3D printing materials, such as TPU, ABS, PETG, and PLA. The analysis encompassed compression tests, fatigue analysis, and modal analysis, yielding valuable insights into how these materials respond to varying load conditions. The findings highlighted the advantages of 3D printing, including its capacity to fabricate intricate shapes efficiently and with minimal material wastage. However, it also pointed out that 3D printed materials may fall short in matching the material properties achievable through conventional manufacturing methods. The research underscored the pivotal role of FEA in forecasting and comprehending the behavior of 3D printed components, encompassing aspects like deformation, stress distribution, fatigue life, and natural frequencies. Furthermore, it stressed the importance of selecting the appropriate materials to attain desired performance characteristics.

REFERENCES

[1] **[1]** Marcus Ritland (Author) 2014. 3D Printing with Sketchup. Published, Published by Packt Publishing Ltd. Birmingham, UK; ISBN 978-1-78328-457-3.

[2] S. Torta and J. Torta (Author) 2019. 3D Printing: An Introduction. Publisher: David Pallai Mercury learning and information dulles, Virginia Boston, Massachusetts; ISBN-13, 978-1683922094.

[3] Ben Redwood, Filemon Schoffer & Brian Garret (Author) 2017. 3D Hubs B.V. Amsterdam, The Netherlands The 3D Printing Handbook. Book printed by Coers & Roest; 3D Hubs B.V.

[4] https://www.core77.com/posts/71173/How-To-Find-the-Best-3D-Printing-Material-for-Your-Designs

[5] Binbin He et al. 2022. 3D printed biomimetic epithelium/stroma bilayer hydrogel implant for corneal regeneration. Bioactive Materials, 17, 234–247; https://doi.org/10.1016/j.bioactmat.2022.01.034.

[6] Chao Bao et al. 2022. A 3D-printed neuromorphic humanoid hand for grasping unknown objects. Article iScience, 25, 104119, https://doi.org/10.1016/j.isci.2022.104119.

[7] Farah Syazwani Shahar et al 2022. Fatigue and impact properties of 3D printed PLA reinforced with kenaf particles. journal of materials researchand technology, 16, 461-470 https://doi.org/10.1016/j.jmrt.2021.12.023.

[8] Irina Ivanova et al 2022. Comparison between methods for indirect assessment of buildability in fresh 3D printed mortar and concrete. Results in Engineering, 13, 100372; https://doi.org/10.1016/j.rineng.2022.100372.

[9] Philippe Lesage et al 2022. Mechanical characterization of 3D printed samples under vibration: Effect of printing orientation and comparison with subtractive manufacturing. Results in Engineering, 13, 100372; https://doi.org/10.1016/j.rineng.2022.100372.

[10] Saquib Rouf et al 2022. 3D printed parts and mechanical properties: Influencing parameters, sustainability aspects, global market scenario, challenges and applications. Advanced Industrial and Engineering Polymer Research Accepted. https://doi.org/10.1016/j.aiepr.2022.02.001.

[11] Su Hyun Lee et al 2022. Plaque removal effectiveness of 3D printed dental hygiene chews with various infill structures through artificial dogteeth. Heliyon, 8, e09096;https://doi.org/10.1016/j.heliyon.2022.e09096.

[12] A.K. Haldar et al 2021, Compressive behaviour of 3D printed sandwich structures based on corrugated core design. Materials Today Communications, Accepted ; https://doi.org/10.1016/j.mtcomm.2020.101725.